

Research Article

Impact of Overlapping Fe/TiO₂ Prepared by Sol-Gel and Dip-Coating Process on CO₂ Reduction

Akira Nishimura,¹ Xuyan Zhao,¹ Takuya Hayakawa,¹ Noriaki Ishida,¹
Masafumi Hirota,¹ and Eric Hu²

¹*Division of Mechanical Engineering, Graduate School of Engineering, Mie University, 1577 Kurimamachiya-cho, Tsu, Mie 514-8507, Japan*

²*School of Mechanical Engineering, The University of Adelaide, Adelaide, SA 5005, Australia*

Correspondence should be addressed to Akira Nishimura; nisimura@mach.mie-u.ac.jp

Received 22 March 2016; Accepted 31 May 2016

Academic Editor: Meenakshisundaram Swaminathan

Copyright © 2016 Akira Nishimura et al. This is an open access article distributed under the Creative Commons Attribution License, which permits unrestricted use, distribution, and reproduction in any medium, provided the original work is properly cited.

Fe-doped TiO₂ (Fe/TiO₂) film photocatalyst was prepared by sol-gel and dip-coating process to extend its photoresponsivity to the visible spectrum. To promote the CO₂ reduction performance with the photocatalyst, some types of base materials used for coating Fe/TiO₂, which were netlike glass fiber and Cu disc, were investigated. The characterization of prepared Fe/TiO₂ film coated on netlike glass fiber and Cu disc was analyzed by SEM and EPMA. In addition, the CO₂ reduction performance of Fe/TiO₂ film coated on netlike glass disc, Cu disc, and their overlap was tested under a Xe lamp with or without ultraviolet (UV) light, respectively. The results show that the concentration of produced CO increases by Fe doping irrespective of base material used under the illumination condition with UV light as well as that without UV light. Since the electron transfer between two overlapped photocatalysts is promoted, the peak concentration of CO for the Fe/TiO₂ double overlapping is approximately 1.5 times as large as the Fe/TiO₂ single overlapping under the illumination condition with UV light, while the promotion ratio is approximately 1.1 times under that without UV light.

1. Introduction

Due to mass consumption of fossil fuels, global warming and fossil fuels depletion have become serious global environmental problems in the world. After the industrial revolution, the averaged concentration of CO₂ in the world has been increased from 278 ppmV to 396 ppmV by 2013 [1]. Therefore, it is necessary to develop a new CO₂ reduction or utilization technology in order to recycle CO₂.

According to the review of CO₂ conversion technologies [2], there are six vital CO₂ conversions: chemical conversions, electrochemical reductions, biological conversions, reforming, inorganic conversions, and photochemical reductions [3]. Recently, artificial photosynthesis or the photochemical reduction of CO₂ to fuel has become an attractive route due to its economically and environmentally friendly behavior [2].

TiO₂ is the principle catalyst for almost all types of photocatalysis reaction. It is well known that CO₂ can be

reduced into fuels, for example, CO, CH₄, CH₃OH, and H₂, and so forth by using TiO₂ as the photocatalyst under ultraviolet (UV) light illumination [4–9]. If this technique could be applied practically, a carbon circulation system would then be established: CO₂ from the combustion of fuel is reformed to fuels again using solar energy, and true zero emission can be achieved. However, the CO₂ reduction performance of TiO₂ is still low. One of the barriers to realization of carbon circulation system utilizing solar energy is that TiO₂ is only photoactive at the wavelength below 400 nm due to its relatively large band gap energy (~3.2 eV) [10].

Recently, studies on CO₂ photochemical reduction by TiO₂ have been carried out from the viewpoint of performance promotion by extending absorption range towards visible region [11–15]. Noble metal doping such as Pt, Pd, Rh, Au, and Ag [11], nanocomposite CdS/TiO₂ combining two different band gap photocatalysts [12], N₂ modified TiO₂

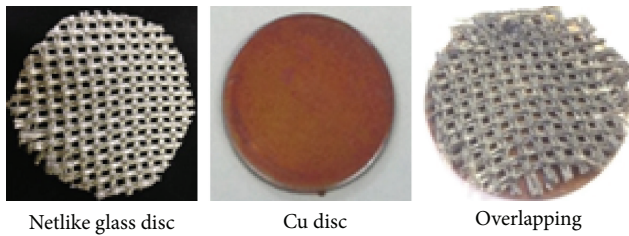


FIGURE 1: The base materials used for coating TiO_2 film.

[13], light harvesting complex of green plants assisted Rh-doped TiO_2 [14], and dye sensitized TiO_2 [15] have been developed for this process. However, the concentration in the products achieved in all the attempts so far is still low, ranging from 10 ppmV to 1000 ppmV [4, 6–9] or from $1 \mu\text{mol/g-cat}$ to $100 \mu\text{mol/g-cat}$ [11–15]. Therefore, the big breakthrough in increasing the concentration level of products is necessary to advance the CO_2 reduction technology in order to make the technology practically useful.

In the present paper, TiO_2 sol-gel and dip-coating process with doping is adopted in order to extend its photoresponsivity to the visible spectrum to promote the CO_2 reduction performance. This process can incorporate dopants into TiO_2 lattice, resulting in the better optical and catalytic properties [16]. In addition, the integration of dopants into the sol during the gelation process facilitates direct interaction between TiO_2 and dopants during the sol-gel process [17].

It was reported that doping transition metal was a useful technique for extending the absorbance of TiO_2 into the visible region [18]. For doping, various metal ions have been used, but among them, Fe^{3+} is considered as a strong candidate as it has a similar radius to Ti^{4+} ($\text{Fe}^{3+} = 78.5 \text{ pm}$, $\text{Ti}^{4+} = 74.5 \text{ pm}$) [19] and can easily fit into the crystal lattice of TiO_2 [18, 20, 21]. Moreover, the redox potential (energy differential) of $\text{Fe}^{2+}/\text{Fe}^{3+}$ is close to that of $\text{Ti}^{3+}/\text{Ti}^{4+}$, resulting in shifting its optical absorption into the visible region [18, 20, 21]. Due to easy availability as well as the above described characteristics, Fe is selected as the dopant in the present study.

In the present paper, a net glass fiber (SILIGLASS U, Nihonmuki Co.) and Cu disc are used as base material for coating TiO_2 film by sol-gel and dip-coating process. Figure 1 shows the netlike glass disc, Cu disc, and two overlapped base materials. The netlike glass fiber is a net composed of glass fiber whose diameter is about $10 \mu\text{m}$. The fine glass fibers are knitted, resulting in the fact that the diameter of aggregate fiber is about 1 mm. According to manufacture specifications of netlike glass fiber, the porous diameter of glass fiber is about 1 nm and the specific surface area is about $400 \text{ m}^2/\text{g}$. The netlike glass fiber consists of SiO_2 whose purity is over 96 wt%. The aperture of net is about $2 \text{ mm} \times 2 \text{ mm}$. Since the netlike glass fiber has a porous characteristic, it is believed that TiO_2 film and doped metal are captured by netlike glass fiber easily during sol-gel and dip-coating process. In addition, it can be expected that a CO_2 absorption performance of prepared photocatalyst is promoted due to the porous structure of netlike glass fiber. On the other hand, Cu disc is also adopted since the recombination of

electron and hole produced by photochemical reaction can be prevented by a free electron emitted from Cu disc. The coupling effect of prepared photocatalysts coated on overlapped netlike glass fiber and Cu disc on CO_2 reduction performance is investigated. The illumination light is able to penetrate through the netlike glass fiber and reach on Cu disc. If the synergy effect between the photocatalyst coated on netlike glass fiber and that on Cu disc was obtained due to an active electron transfer between them, the promotion of CO_2 reduction performance would be achieved. There is no previous study on the coupling effect on CO_2 reduction performance of metal doped TiO_2 or nondoped TiO_2 .

In the present paper, TiO_2 film doped with Fe (Fe/TiO_2) was prepared and characterized by Scanning Electron Microscope (SEM) and Electron Probe Micro Analyzer (EPMA) analysis. The CO_2 reduction characteristics of Fe/TiO_2 coated on net glass fiber and/or Cu disc under the condition of illuminating Xe lamp with or without UV light were investigated.

2. Experiment

2.1. Preparation of Fe/TiO_2 Film. Sol-gel and dip-coating process was used for preparing Fe/TiO_2 film in this study. TiO_2 sol solution was made by mixing $[(\text{CH}_3)_2\text{CHO}]_4\text{Ti}$ (purity of 95 wt%, Nacalai Tesque Co.) of 0.3 mol, anhydrous $\text{C}_2\text{H}_5\text{OH}$ (purity of 99.5 wt%, Nacalai Tesque Co.) of 2.4 mol, distilled water of 0.3 mol, and HCl (purity of 35 wt%, Nacalai Tesque Co.) of 0.07 mol. Fe powders (Merck KGaA, particle size below $10 \mu\text{m}$) were added to TiO_2 sol solution. Netlike glass fiber was cut to disc, and its diameter and thickness were 50 mm and 1 mm, respectively. The Cu disc used has diameter and thickness of 50 mm and 1 mm, respectively. The base material was dipped into Fe/TiO_2 sol solution at the speed of 1.5 mm/s and pulled up at the fixed speed of 0.22 mm/s. Then, it was dried out and fired under the controlled firing temperature (FT) and firing duration time (FD), resulting in the fact that Fe/TiO_2 film was fastened on the base material. FT and FD were set at 623 K and 180 s, respectively. The ratio of amount of added Fe to amount of TiO_2 sol solution (R) was set at 10 wt%.

2.2. Characterization of Fe/TiO_2 Film. The surface structure and crystallization characteristics of Fe/TiO_2 film were evaluated by SEM (JXA-8530F, JEOL Ltd.) and EPMA (JXA-8530F, JEOL Ltd.). Since these two measuring instruments use electron for analysis, the sample should be an electron conductor. Though Cu disc is a good electron conductor, netlike glass disc is not an electron conductor. In this study, the carbon vapor deposition was conducted by the dedicated device (JEE-420, JEOL Ltd.) for Fe/TiO_2 coated on netlike glass disc before analysis by SEM and EPMA. The thickness of carbon deposited on sample was approximately 20–30 nm. The electron probe emits the electron to the sample under the acceleration voltage of 15 kV and the current of $3.0 \times 10^{-8} \text{ A}$; the surface structure of sample is analyzed by SEM. The characteristic X-ray is detected by EPMA at the same time, resulting in the fact that the concentration of chemical

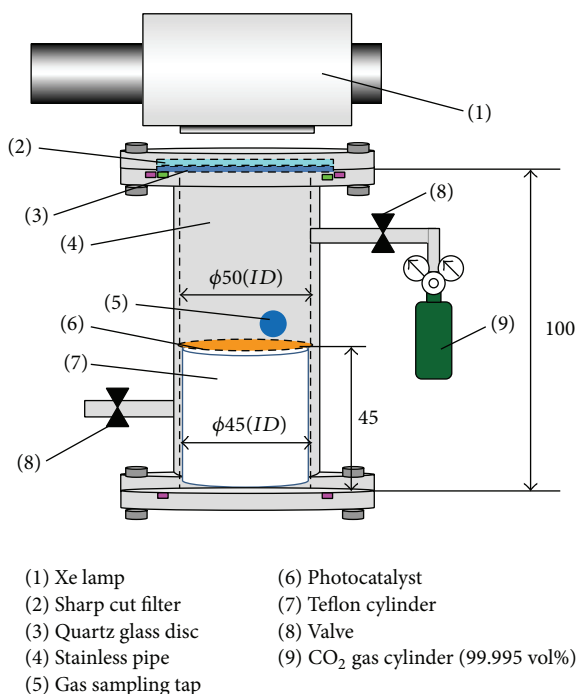


FIGURE 2: Schematic drawing of CO₂ reduction experimental set-up.

element is analyzed according to the relationship between the characteristic X-ray energy and the atomic number. The spatial resolution of SEM and EPMA is 10 μm . The EPMA analysis helps not only to understand the coating state of prepared photocatalyst but also to measure the amount of doped metal within TiO₂ film on the base material.

2.3. CO₂ Reduction Experiment. Figure 2 shows that experimental set-up of the reactor consisting of stainless pipe (100 mm (*H.*) \times 50 mm (*ID*)), a netlike glass disc or Cu disc (50 mm (*D.*) \times 1 mm (*t.*)) coated with Fe/TiO₂ film which is located on the Teflon cylinder (50 mm (*H.*) \times 50 mm (*D.*)), a quartz glass disc (84 mm (*D.*) \times 10 mm (*t.*)), a sharp cut filter which cuts off the light of wavelength below 400 nm (SCF-49.5C-42L, SIGMA KOKI Co. Ltd.), Xe lamp (L2175, Hamamatsu Photonics K.K.), and CO₂ gas cylinder.

The reactor volume available for CO₂ charge is $1.25 \times 10^{-4} \text{ m}^3$. The light of Xe lamp, through the sharp cut filter and the quartz glass disc that are at the top of the stainless pipe, illuminates the netlike glass disc or Cu disc coated with Fe/TiO₂ film, which is located inside the stainless pipe. The wavelength of light from Xe lamp is ranged from 185 nm to 2000 nm. The Xe lamp can be fitted with a sharp cut filter to remove UV components of the light. With the filter, the wavelength of light from Xe lamp is ranged from 401 nm to 2000 nm. Figure 3 shows the light transmittance data of the sharp cut filter to prove the removal of the light whose wavelength is below 400 nm. The average light intensity of Xe lamp on the photocatalyst without and with setting the sharp cut filter is 81.9 mW/cm² and 60.7 mW/cm², respectively.

In the CO₂ reduction experiment, CO₂ gas with the purity of 99.995 vol% was flowed through the reactor as a purged gas

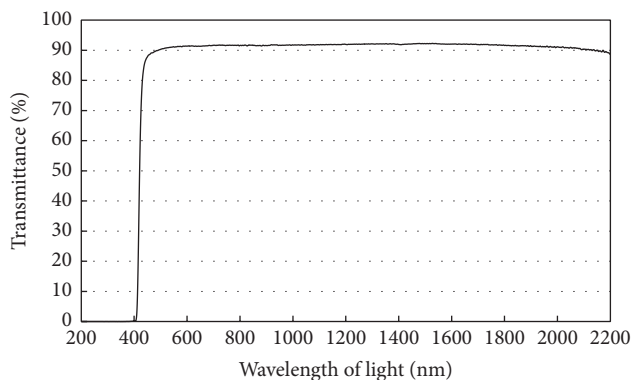


FIGURE 3: Light transmittance data of sharp cut filter.

for 15 minutes first. After that, the valves located at the inlet and the outlet of reactor were closed. After confirming the gas pressure and gas temperature in the reactor at 0.1 MPa and 298 K, respectively, the distilled water of 100 μL was injected into the reactor and Xe lamp illumination was turned on at the same time. The water injected vaporized completely in the reactor. Due to the heat of Xe lamp, the temperature in reactor was attained at 343 K within an hour and kept at approximately 343 K during the experiment. The amount of injected water and that of CO₂ in the reactor were 5.56 mmol and 5.76 mmol, respectively. The gas in the reactor was sampled every 24 hours during the experiment. The gas samples were analyzed by FID gas chromatograph (GC353B, GL Science) and methanizer (MT221, GD Science). Minimum resolution of FID gas chromatograph and methanizer is 1 ppmV.

3. Results and Discussion

3.1. Characterization of Fe/TiO₂ Film by SEM and EPMA. Figures 4 and 5 show SEM images of TiO₂ and Fe/TiO₂ film coated on netlike glass disc, respectively. The SEM images were taken at 1500 times magnification under the acceleration voltage of 15 kV and the current of $3.0 \times 10^{-8} \text{ A}$.

Figures 6 and 7 show EPMA images of TiO₂ and Fe/TiO₂ film coated on netlike glass disc, respectively. EPMA analysis was carried out for 1500 times magnification SEM images shown in Figures 4 and 5. In EPMA image, the concentrations of each element in observation area are indicated by the different colors. Light colors, for example, white, pink, and red, indicate that the amount of element is large, while dark colors like black and blue indicate that the amount of element is small.

To identify the position of each element, the colored circles are added to these SEM and EPMA images. The red circles shown in SEM images of Figures 4 and 5 indicate the amount of Ti is large as pointed out in EPMA images of Figures 6 and 7. From these figures, it can be observed that TiO₂ film with teeth-like shape is coated on netlike glass fiber. It is also seen that TiO₂ film builds a bridge among several glass fibers. During firing process, the temperature profile of TiO₂ solution adhered on the netlike glass disc is not even due to the difference of thermal conductivities of

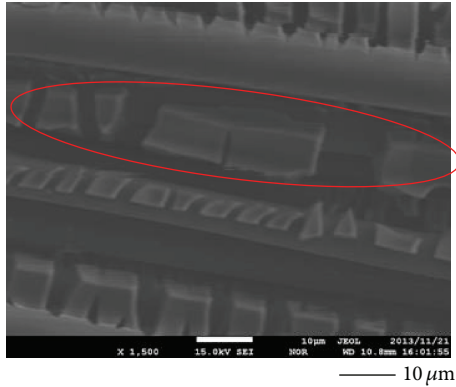


FIGURE 4: SEM image of TiO_2 film coated on netlike glass disc.

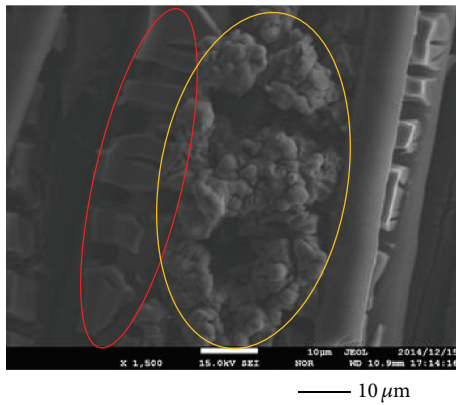


FIGURE 5: SEM image of Fe/TiO_2 film coated on netlike glass disc.

Ti and SiO_2 . Thermal conductivities of Ti and SiO_2 at 600 K are $19.4 \text{ W}/(\text{m}\cdot\text{K})$ and $1.82 \text{ W}/(\text{m}\cdot\text{K})$, respectively [22]. Since the thermal expansion and shrinkage around netlike glass fiber occur, thermal crack of TiO_2 film is caused. Therefore, TiO_2 film on netlike glass fiber is teeth-like.

The yellow circle shown in SEM image of Figure 5 indicates the existence of metal particles as pointed out in EPMA images of Figure 7. It is observed from Figure 5 that Fe particles adhere on the netlike glass fiber directly. According to Figure 5, the size of doped metal is below $10 \mu\text{m}$. Since the Fe particles used have diameters below $10 \mu\text{m}$, it is confirmed that the Fe particles can be loaded without agglomeration by the sol-gel and dip-coating process.

Figures 8 and 9 show SEM images of TiO_2 and Fe/TiO_2 film coated on Cu disc, respectively. The SEM images were taken at 1500 times magnification under the acceleration voltage of 15 kV and the current of $3.0 \times 10^{-8} \text{ A}$.

Figures 10 and 11 show EPMA images of TiO_2 and Fe/TiO_2 film coated on Cu disc, respectively. EPMA analysis was carried out for 1500 times magnification SEM images shown in Figures 8 and 9.

To identify the position of each element, the colored circles are added to these SEM and EPMA images. The red circles shown in SEM images of Figures 8 and 9 indicate the TiO_2 film is contracted as also seen in EPMA images

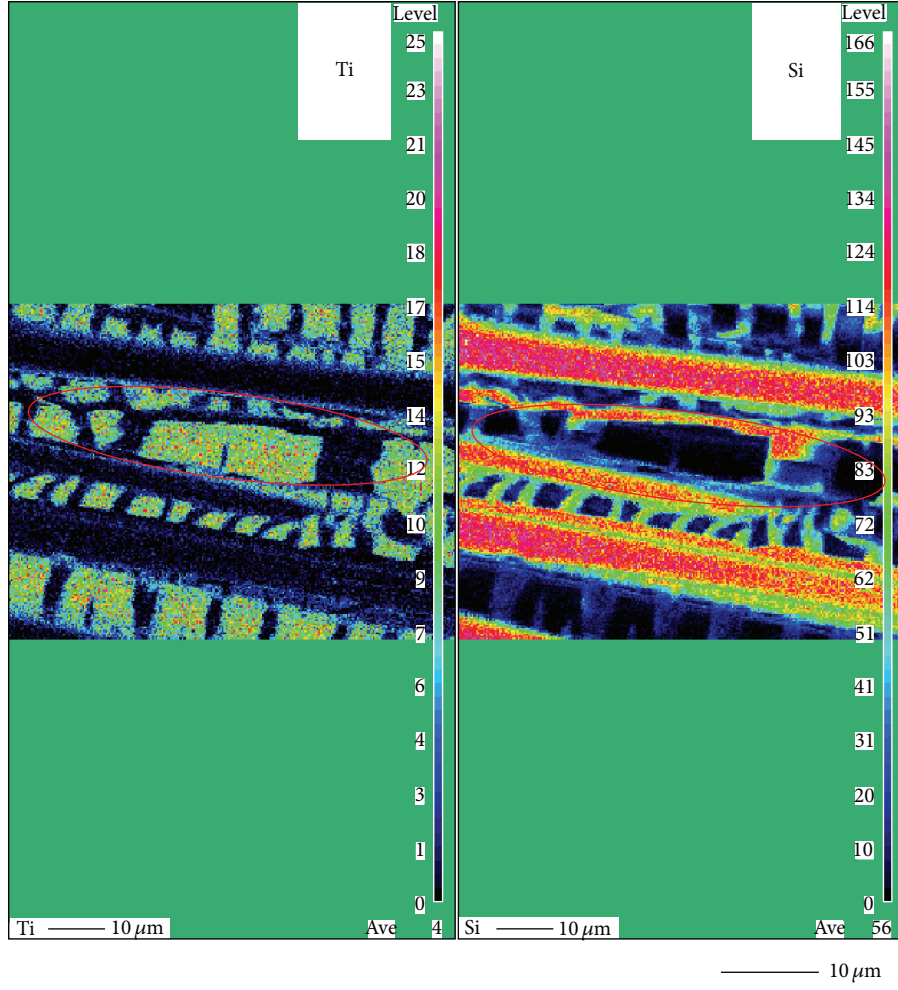
of Figures 10 and 11. The yellow circle in Figure 11 indicates the existence of Fe particles. According to Figures 9 and 11, the TiO_2 film is contracted around Fe particles. The surface characteristics of TiO_2 or Fe/TiO_2 are explained as follows [23]:

- (i) Before firing process, TiO_2 or Fe/TiO_2 sol solution is adhered on Cu disc uniformly.
- (ii) During firing process, the temperature profile of TiO_2 or Fe/TiO_2 sol solution adhered on Cu disc is not even due to the difference of thermal conductivities of Cu, Ti, and Fe. Thermal conductivities of Cu, Ti, and Fe at 600 K are $383 \text{ W}/(\text{m}\cdot\text{K})$, $19.4 \text{ W}/(\text{m}\cdot\text{K})$, and $54.7 \text{ W}/(\text{m}\cdot\text{K})$, respectively [22]. Therefore, the thermal expansion around Fe particles and the thermal shrinkage around the other areas of TiO_2 sol occur for Fe/TiO_2 , while the thermal expansion and shrinkage between TiO_2 and Cu disc occur for nonmetal doped TiO_2 film.
- (iii) Because of thermal stress caused by the uneven distribution of temperature, the cracks around Fe and the shrinkage of TiO_2 film around the cracks occur after firing process. Therefore, a large amount of Cu pointed out by orange circles, which is an element of basis Cu disc, around Fe and a large amount of Ti around Fe are observed in Figure 11.

To evaluate the amount of doped Fe within TiO_2 film quantitatively, the observation area, which is the center of netlike glass disc or Cu disc, of diameter of $300 \mu\text{m}$ is analyzed by EPMA. The ratio of Fe to Ti in this observation area is counted by averaging the data obtained in this area.

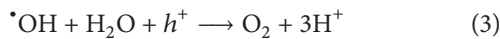
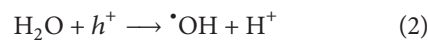
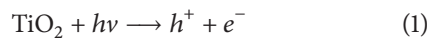
Table 1 gives the weight percentages of elements Fe and Ti in the Fe/TiO_2 film coated on netlike glass disc or Cu disc. From this table, it can be seen that more Fe is contained in the Fe/TiO_2 film on netlike glass disc than that on Cu disc, under the doping condition, that is, R of 10 wt%. As expected, the netlike glass fiber can capture the dopant metal powder well during dip-coating process due to the porous structure. However, Cu disc hardly captures the dopant metal powder during dip-coating process since the surface of Cu disc is smooth. From these results, it is clear that the amount of dopants which could be doped is influenced by the base material when the sol-gel and dip-coating process is adopted for metal doping.

3.2. CO_2 Reduction Characteristics of Fe/TiO_2 Coated on Netlike Glass Disc or Cu Disc. Figure 12 shows the concentration changes of CO produced in the reactor along the time under the Xe lamp with UV light on, for TiO_2 or Fe/TiO_2 film coated on netlike glass disc or Cu disc or their overlap. In this figure, a single overlapping means the photocatalyst coated on the upper surface of netlike glass disc is overlapped over the photocatalyst coated on Cu disc, while a double overlapping means the photocatalyst coated on both the upper and lower surfaces of netlike glass disc is overlapped over the photocatalyst coated on Cu disc. In this experiment, CO is the only fuel produced from the reactions. The reaction

FIGURE 6: EPMA image of TiO₂ film coated on netlike glass disc.TABLE 1: Weight ratio of elements Fe and Ti within prepared metal doped TiO₂ film.

Photocatalyst type	Weight ratio		
	Ti (wt%)	Fe (wt%)	Total (wt%)
Fe/TiO ₂ coated on netlike glass disc	74.76	25.24	100.00
Fe/TiO ₂ coated on Cu disc	98.15	1.85	100.00

scheme for CO production by the photochemical reaction with CO₂ and H₂O is shown as follows [4, 7, 24–26]:



Since the concentrations of CO in most experiments started to decrease after illumination of 48–72 hours for illumination conditions with UV light due to the reverse reaction by CO and O₂ which is by-product as shown in (3), Figure 12 only shows the concentration up to 72 hours. Before the experiments, a blank test, which was running the same experiment without illumination of Xe lamp, had been carried out to set up a reference case. No fuel was produced in the blank test as expected.

According to Figure 12, the concentration of CO increases due to Fe doping irrespective of base material. The improvement of photocatalytic performance by Fe doping under the illumination condition with UV light can be caused by the generation of shallow charge traps in the crystal structure which decreases the recombination rate of electron-hole pairs [20]. In addition, the concentration of CO produced by Fe/TiO₂ coated on Cu disc is higher than that on netlike glass disc. Though the weight ratio of Fe for Fe/TiO₂ coated on netlike glass disc is larger than that on Cu disc as shown in Table 1, the reaction surface area which can receive

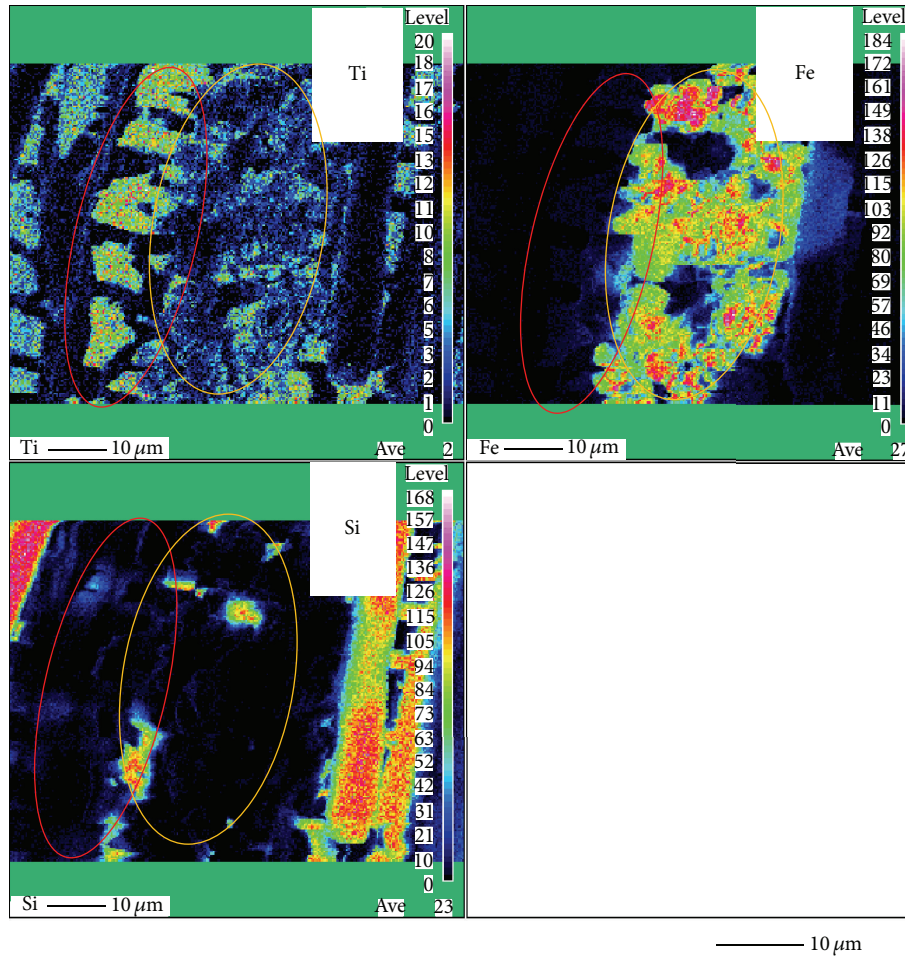


FIGURE 7: EPMA image of Fe/TiO₂ film coated on netlike glass disc.

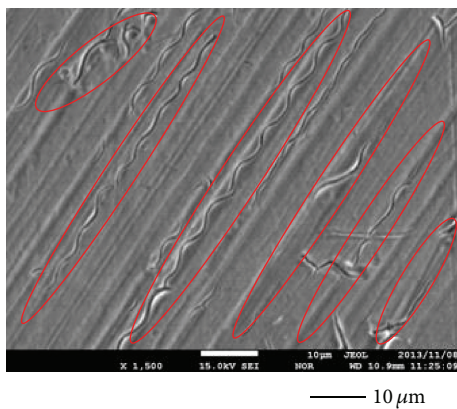


FIGURE 8: SEM image of TiO₂ film coated on Cu disc.

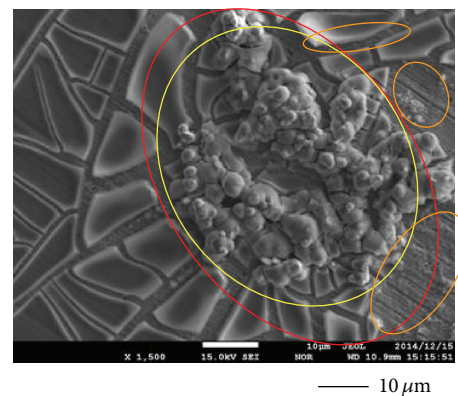


FIGURE 9: SEM image of Fe/TiO₂ film coated on Cu disc.

the light is small due to aperture of net. Therefore, the photocatalytic performance of Fe/TiO₂ coated on netlike glass disc is lower than that on Cu disc. Moreover, the Fe/TiO₂ single overlapping shows the small superiority over Fe/TiO₂ coated on netlike glass disc and Fe/TiO₂ coated on Cu disc. Although the present study expected the positive

synergy effect of combination of two photocatalysts coated on different base materials, the positive effect observed was very small. Since the netlike glass fiber consists of SiO₂ which is an electrical insulation material, the electron transfer between two overlapped photocatalysts might not be realized well. However, in the experiment of the Fe/TiO₂ double

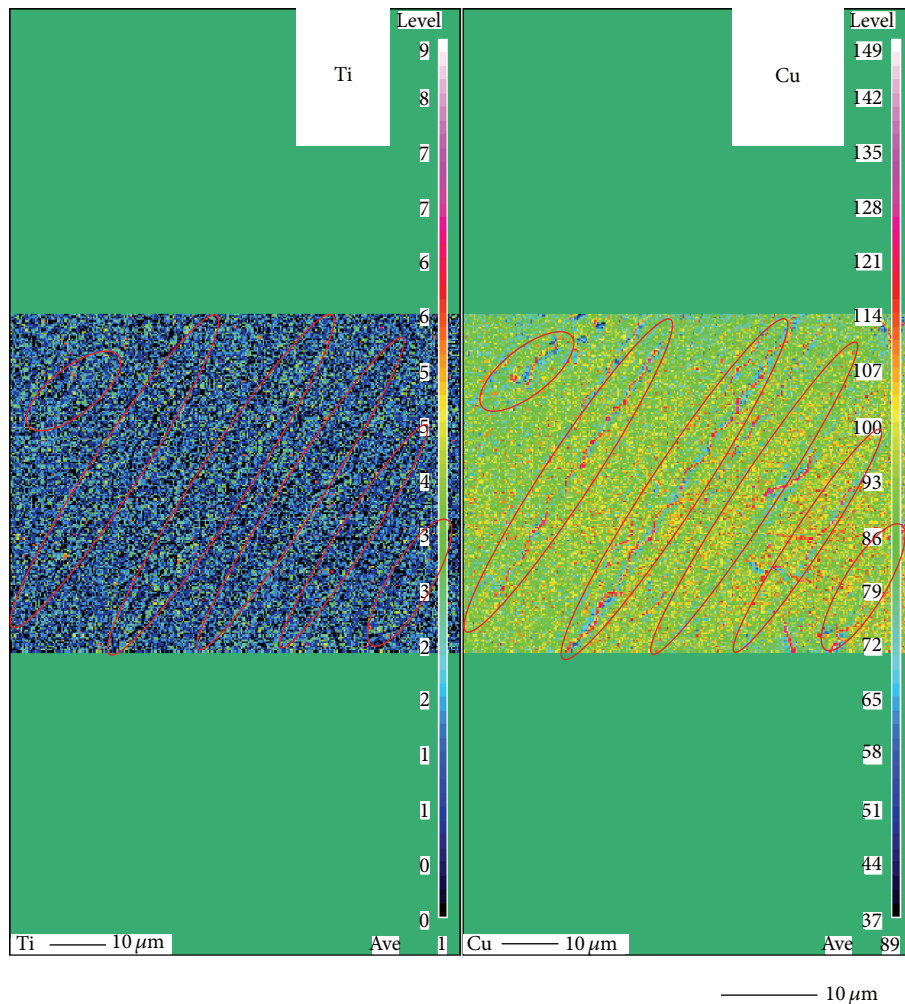


FIGURE 10: EPMA image of TiO_2 film coated on Cu disc.

overlapping, the photocatalytic performance is promoted, resulting in the fact that the peak concentration of CO is approximately 1.5 times as large as the Fe/TiO_2 single overlapping. The reason is thought to be that the electron transfer between two overlapped photocatalysts is promoted, resulting in the fact that the synergy effect of combination of two photocatalysts coated on different base materials is obtained.

Figure 13 illustrates the difference of electron transfer phenomenon between single and double overlapping. In this figure, the hole produced by photochemical reaction is not shown to clarify the electron transfer phenomenon mainly. It is believed that the path for electron transfer is constructed by double overlapping.

Figure 14 shows the comparison of molar quantities of CO per weight of photocatalyst among prepared photocatalysts. These values are estimated based on the maximum CO obtained under the illumination condition with UV light up to 72 hours. According to this figure, the molar quantity of CO per weight of Fe/TiO_2 coated on Cu disc shows the highest performance since the weight of Fe/TiO_2 coated on Cu disc ($= 0.02 \text{ g-cat}$) is smaller than that on netlike glass disc

($= 0.25 \text{ g-cat}$). Though the netlike glass fiber captures the large amount of TiO_2 sol and Fe particle during dipping process well, some Fe/TiO_2 adhered in the pore of netlike glass fiber might not be activated well due to lack of light illumination. Although it is believed that the doping of Fe could assist CO_2 reduction if the light could illuminate inside the pore of netlike glass disc, the positive effect of Fe doping on CO_2 reduction performance per weight of photocatalyst base under the overlapping condition was not as significant as that in the case of Fe/TiO_2 coated on netlike glass disc. In addition, the mass transfer in the space between two photocatalysts coated on netlike glass disc and Cu disc should be enhanced in order to meet the photoreaction rate under the overlapping condition. If the produced fuel remains in the space between two photocatalysts, the reactant of CO_2 and H_2O could be blocked to reach the surface of photocatalyst, resulting in the fact that the photochemical reaction could not be carried out well even though the light is illuminating for photocatalyst. Therefore, it is necessary to control the amount of doped Fe which is coated on the surface and on the pore of the netlike glass fiber while also optimizing the aperture of netlike glass fiber.

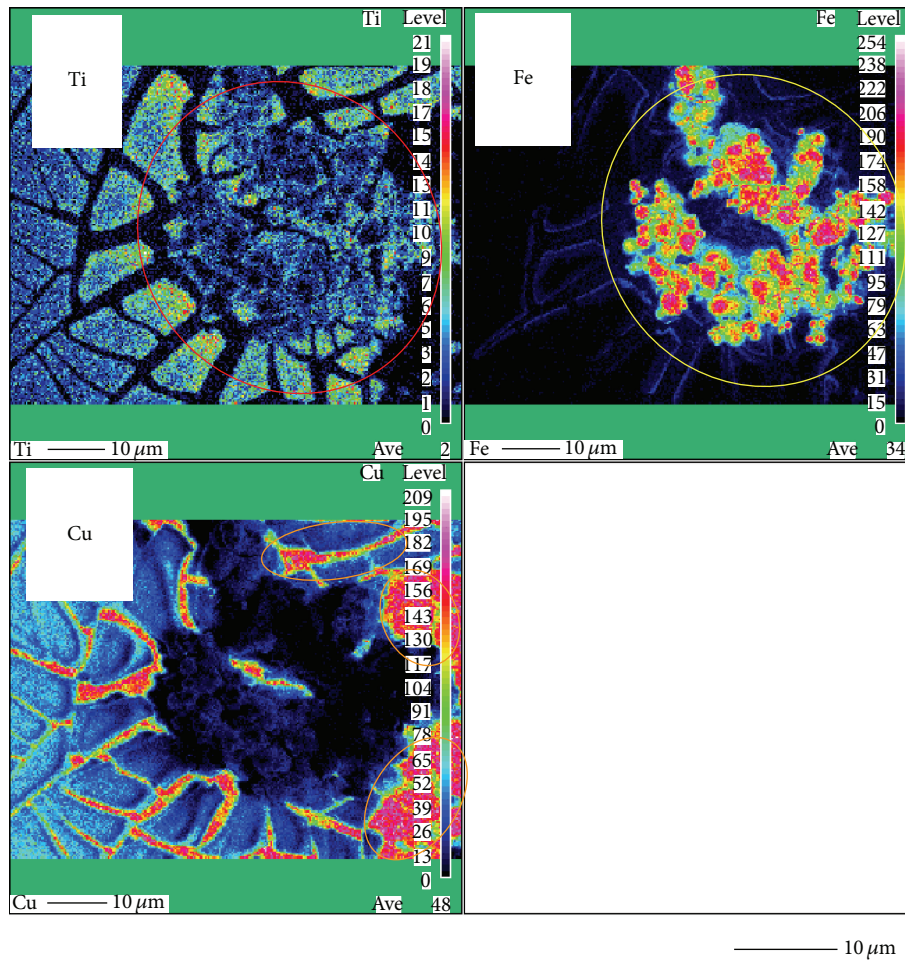


FIGURE 11: EPMA image of Fe/TiO₂ film coated on Cu disc.

Figure 15 shows the concentration changes of CO produced in the reactor along the time under the Xe lamp illumination without UV light, for TiO₂ or Fe/TiO₂ film coated on netlike glass disc or Cu disc or their overlap. In this experiment, CO is the only fuel produced from the reactions. Since the concentration of CO almost started to decrease after illumination of 72–96 hours for all cases due to the reverse reaction by CO and O₂ which is by-product as shown in (3), Figure 15 only shows the concentration up to 96 hours.

From Figure 15, it can be seen that the CO₂ reduction performance of TiO₂ is promoted by Fe doping due to extension of the photoresponsivity of TiO₂ to the visible spectrum as well as decrease in the recombination rate of electron-hole pairs by the generation of shallow charge traps in the crystal structure. In addition, the maximum concentration of CO obtained by Fe/TiO₂ coated on netlike glass disc is almost the same as that by Fe/TiO₂ coated on Cu disc, which is different tendency from the results obtained under the UV illumination condition. Under the illumination condition without UV light, it is believed that the amount of doped Fe is important to absorb the visible light to perform the photocatalytic reaction. Since the amount of doped Fe for Fe/TiO₂ coated on netlike glass disc is much larger than that

for Fe/TiO₂ coated on Cu disc as shown in Table 1, the CO₂ reduction performance of Fe/TiO₂ coated on netlike glass disc equals that on Cu disc, while that on netlike glass disc is lower than that on Cu disc under the illumination condition with UV light.

Furthermore, according to Figure 15, the positive effect of overlapping is obtained, especially under the double overlapping condition. As mentioned before, since the netlike glass fiber consists of SiO₂ which is an electrical insulation material, the electron transfer between two overlapped photocatalysts might not be realized well. However, the photocatalytic performance is promoted up to approximately 1.1 times by double overlapping when the maximum concentrations of CO are compared between the single and the double overlapping condition. The electron transfer between two overlapped photocatalysts is promoted by double overlapping. However, compared to the previous cases with UV illumination, the improvement by double overlapping is small. Since the wavelength of illuminating light penetrating through netlike glass disc becomes longer due to losing energy, the electron produced by the Fe/TiO₂ coated on Cu disc which is positioned under the netlike glass disc decreases. The range of wavelength of light illuminating after penetrating through

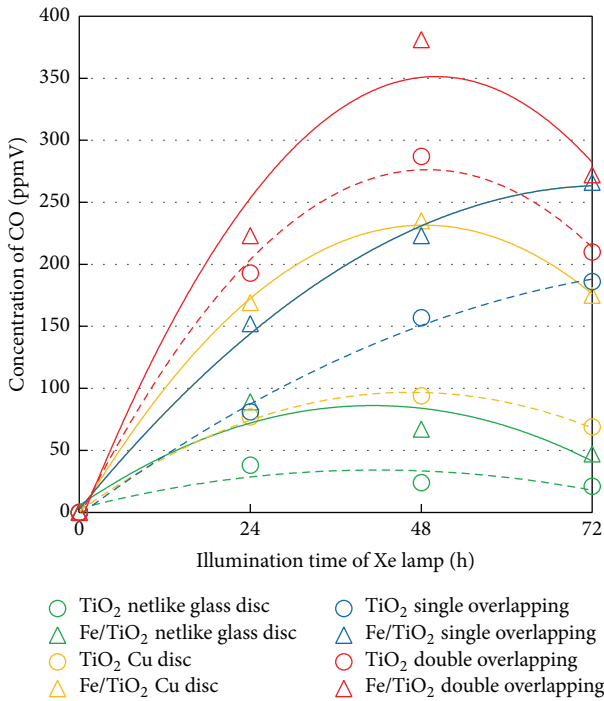


FIGURE 12: Comparison of concentrations of produced CO among photocatalysts coated on different base materials under the illumination condition with UV light.

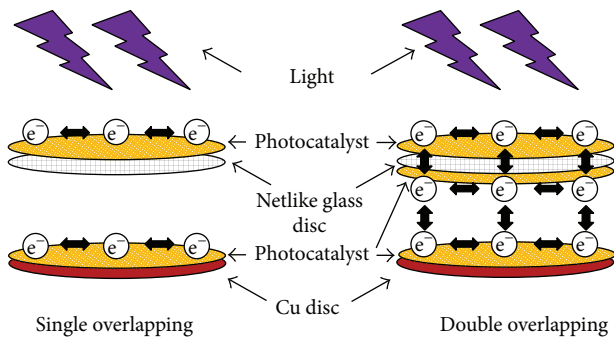


FIGURE 13: Comparison of electron transfer phenomena between single and double overlapping.

netlike glass disc is narrower than that in the UV illumination condition cases. Therefore, the effect of electron transfer promotion between two overlapped photocatalysts is small compared to that in the UV illumination cases.

Figure 16 shows the comparison of molar quantities of CO per weight of photocatalyst among prepared photocatalysts. These values are estimated based on the maximum CO obtained under the no-UV illumination condition up to 96 hours. It reveals that the molar quantity of CO per weight of Fe/TiO₂ under the double overlapping condition is the highest among all experimental conditions. In addition, it also reveals the positive effect of overlapping on CO₂ reduction performance in terms of molar quantity of CO per weight of photocatalyst is achieved in both single and double overlapping cases. It is believed that Fe/TiO₂ coated

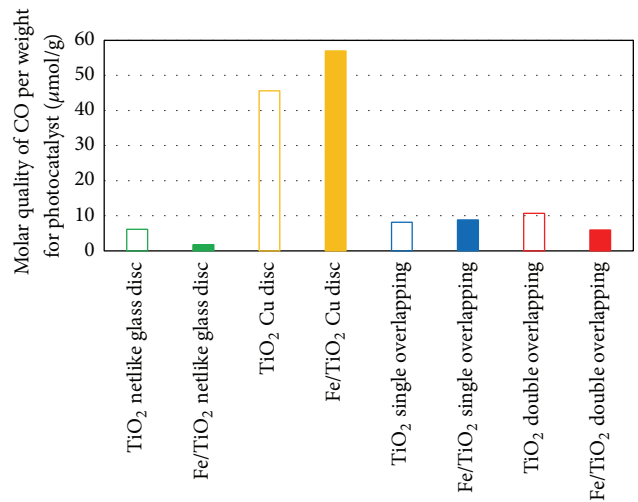


FIGURE 14: Comparison of CO₂ reduction performances per weight of photocatalyst under the illumination condition with UV light.

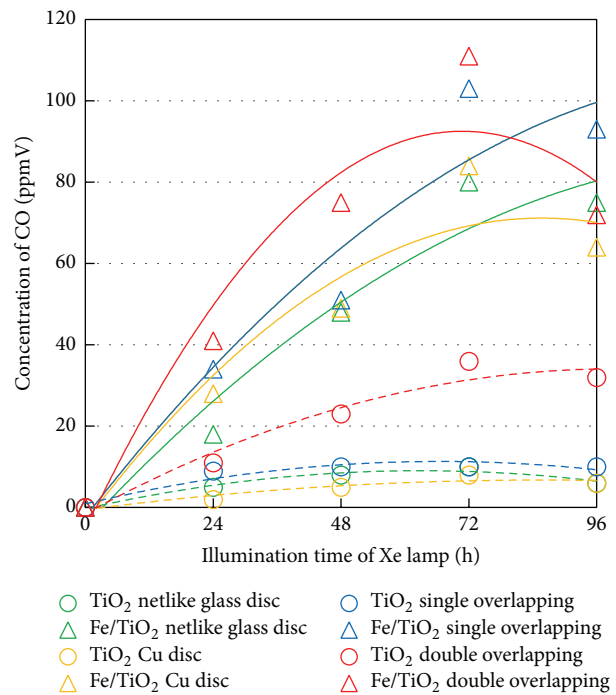


FIGURE 15: Comparison of concentrations of produced CO among photocatalysts coated on different base materials under the illumination condition without UV light.

on Cu disc, which is positioned under the netlike glass disc, can utilize at least some of the light penetrating through the aperture of netlike glass disc for photochemical reaction, although the wavelength of the penetrating light becomes long.

The bigger synergy effect in terms of molar quantity of CO per weight of photocatalyst for two overlapped photocatalysts in no-UV cases is achieved when comparing with UV illumination cases. Since the photochemical reaction rate and the amount of produced fuel are small under

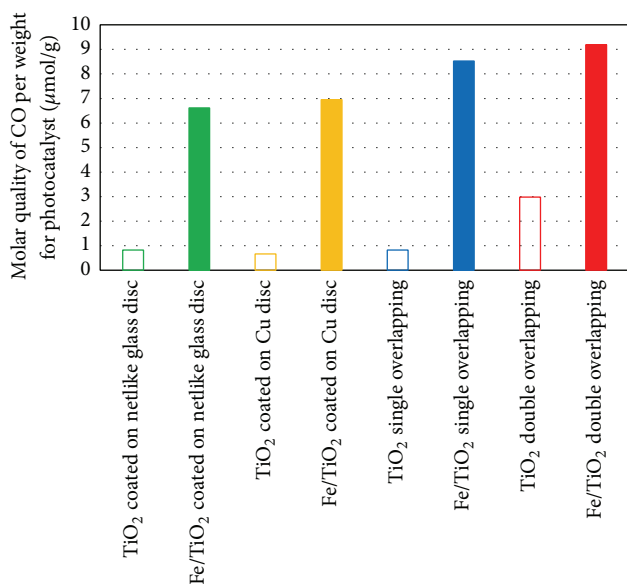


FIGURE 16: Comparison of CO₂ reduction performances per weight of photocatalyst under the illumination condition without UV light.

the no-UV illumination condition compared to those with UV light, it would be beneficial to the mass transfer between produced fuel and reactant of CO₂ and H₂O on the surface of photocatalyst in no-UV cases. As a result, the mass transfer and photochemical reaction are carried out effectively in no-UV cases. Therefore, the molar quantity of CO per weight of photocatalyst for overlapping cases is large in no-UV cases. According to the previous reports [27, 28], the mass transfer is an inhibition factor to promote the CO₂ reduction performance of photocatalyst and it is necessary to control the mass transfer rate to meet the photochemical reaction rate. Figure 17 illustrates the comparison of mass and electron transfer within two overlapped photocatalysts in UV and no-UV illumination cases.

Compared to the previous researches [4, 6–9, 11–15], the CO₂ reduction performance of photocatalysts prepared in the present study is almost at the same level. However, the present study clarifies that the double overlapping arrangement is effective in improving CO₂ reduction performance of Fe/TiO₂. It therefore proposes that the netlike porous metal having an appropriate area of aperture can be a good base material for overlapping arrangement instead of netlike glass fiber since the former has good electrical conductivity, light permeability, and gas diffusivity. In addition, the dopant like Cu, which can absorb the longer wavelength light than Fe [21], should be used in the layers at lower positioned photocatalysts in overlapping conditions. This proposal is similar to the concept of the hybrid photocatalyst using two photocatalysts having different band gaps [29–31].

Though this study has not confirmed about the magnetic properties of the prepared Fe/TiO₂ experimentally, some references reported the ferromagnetic characteristic of Fe/TiO₂ [32–34]. However, the amount of doped Fe was small, which was below 6 wt% [32, 34]. In addition, it was reported that the characteristic changed to the paramagnetic one with rising of

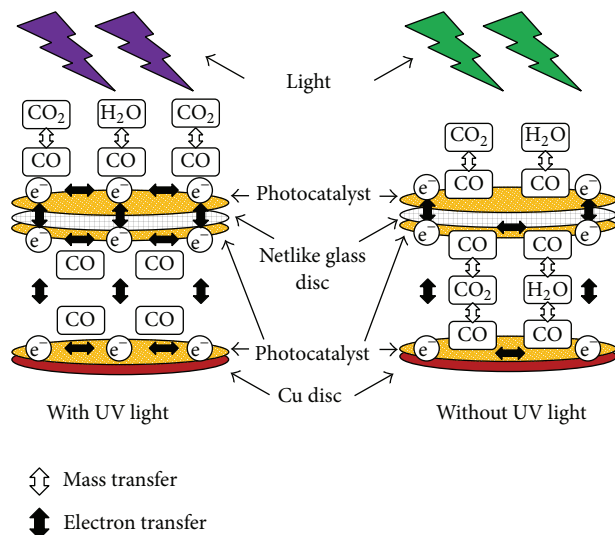


FIGURE 17: Comparison of mass and electron transfer within two overlapped photocatalysts between the illumination condition with UV light and that without UV light.

Fe content [32]. Furthermore, it was also reported that the ferromagnetic behavior was observed for Fe/TiO₂ annealed in vacuum at room temperature, while the ferromagnetic behavior was not observed for Fe/TiO₂ without annealing [33]. In this study, the amount of doped Fe for Fe/TiO₂ on netlike glass disc and that on Cu disc were 25.24 wt% and 1.85 wt%, respectively, according to Table 1, while the amount of doped Fe was set at 10 wt% and the annealing treatment was not carried out. Though it is necessary to investigate the prepared Fe/TiO₂ by magnetic properties measurement system in the near future, this study supposes that the magnetism of prepared Fe/TiO₂ on net glass disc is low.

4. Conclusions

Based on the investigation by this study, the following conclusions can be drawn:

- (1) TiO₂ film with teeth-like shape could be coated on netlike glass fiber and Fe fine particles are loaded without agglomeration. However, TiO₂ film would contract around Fe particles when Fe/TiO₂ was coated on Cu disc.
- (2) The amount of dopants that could be coated is influenced by the base material used.
- (3) Under the UV illumination condition, the concentration of produced CO increases due to Fe doping irrespective of base material used. The photocatalytic performance of using Fe/TiO₂ coated on netlike glass disc is lower than that on Cu disc. The peak concentration of CO for the Fe/TiO₂ double overlapping is approximately 1.5 times as large as the Fe/TiO₂ single overlapping.
- (4) Under the illumination condition without UV light, the CO₂ reduction performance of TiO₂ is also

promoted by Fe doping due to extension of the photoresponsivity of TiO₂ to the visible spectrum as well as decrease in the recombination rate of electron-hole pairs by the generation of shallow charge traps in the crystal structure. The positive effect of overlapping is obtained especially under the double overlapping condition. From the viewpoint of the molar quantity of CO per weight of photocatalyst, the Fe/TiO₂ double overlapping shows the highest performance. It is believed that the mass transfer rates between produced fuel and reactants on the surface of photocatalyst are better matched with the photochemical reaction rates when Fe/TiO₂ is double overlapped.

- (5) The double overlapping arrangement is effective for improving the CO₂ reduction performance of Fe/TiO₂.

Competing Interests

The authors declare that there are no competing interests regarding the publication of this paper.

Acknowledgments

The authors would like to gratefully thank JSPS KAKENHI for Grant no. 25420921, Tanikawa Foundation, and Mazda Foundation for the financial support of this work.

References

- [1] World Data Center for Greenhouse Gases, <http://ds.data.jma.go.jp/gmd/wdcgg/wdcgg.html>.
- [2] S. Das and W. M. A. W. Daud, "Photocatalytic CO₂ transformation into fuel: a review on advances in photocatalyst and photoreactor," *Renewable and Sustainable Energy Reviews*, vol. 39, pp. 765–805, 2014.
- [3] T. Sakakura, J.-C. Choi, and H. Yasuda, "Transformation of carbon dioxide," *Chemical Reviews*, vol. 107, no. 6, pp. 2365–2387, 2007.
- [4] K. Adachi, K. Ohta, and T. Mizuno, "Photocatalytic reduction of carbon dioxide to hydrocarbon using copper-loaded titanium dioxide," *Solar Energy*, vol. 53, no. 2, pp. 187–190, 1994.
- [5] M. Anpo and K. Chiba, "Photocatalytic reduction of CO₂ on anchored titanium oxide catalysts," *Journal of Molecular Catalysis*, vol. 74, no. 1–3, pp. 207–212, 1992.
- [6] G. R. Dey, A. D. Belapurkar, and K. Kishore, "Photo-catalytic reduction of carbon dioxide to methane using TiO₂ as suspension in water," *Journal of Photochemistry and Photobiology A: Chemistry*, vol. 163, no. 3, pp. 503–508, 2004.
- [7] K. Hirano, K. Inoue, and T. Yatsu, "Photocatalysed reduction of CO₂ in aqueous TiO₂ suspension mixed with copper powder," *Journal of Photochemistry and Photobiology, A: Chemistry*, vol. 64, no. 2, pp. 255–258, 1992.
- [8] O. Ishitani, C. Inoue, Y. Suzuki, and T. Ibusuki, "Photocatalytic reduction of carbon dioxide to methane and acetic acid by an aqueous suspension of metal-deposited TiO₂," *Journal of Photochemistry and Photobiology A: Chemistry*, vol. 72, no. 3, pp. 269–271, 1993.
- [9] S. Kaneco, H. Kurimoto, Y. Shimizu, K. Ohta, and T. Mizuno, "Photocatalytic reduction of CO₂ using TiO₂ powders in supercritical fluid CO₂," *Energy*, vol. 24, no. 1, pp. 21–30, 1999.
- [10] M. M. Gui, S.-P. Chai, B.-Q. Xu, and A. R. Mohamed, "Enhanced visible light responsive MWCNT/TiO₂ core-shell nanocomposites as the potential photocatalyst for reduction of CO₂ into methane," *Solar Energy Materials & Solar Cells*, vol. 122, pp. 183–189, 2014.
- [11] S. Xie, Y. Wang, Q. Zhang, W. Deng, and Y. Wang, "MgO- and Pt-promoted TiO₂ as an efficient photocatalyst for the preferential reduction of carbon dioxide in the presence of water," *ACS Catalysis*, vol. 4, no. 10, pp. 3644–3653, 2014.
- [12] A. A. Beigi, S. Fatemi, and Z. Salehi, "Synthesis of nanocomposite CdS/TiO₂ and investigation of its photocatalytic activity for CO₂ reduction to CO and CH₄ under visible light irradiation," *Journal of CO₂ Utilization*, vol. 7, pp. 23–29, 2014.
- [13] B. Michalkiewicz, J. Majewska, G. Kadziolka, K. Bubacz, S. Mozia, and A. W. Morawski, "Reduction of CO₂ by adsorption and reaction on surface of TiO₂-nitrogen modified photocatalyst," *Journal of CO₂ Utilization*, vol. 5, pp. 47–52, 2014.
- [14] C.-W. Lee, R. A. Kourouniotti, J. C. S. Wu et al., "Photocatalytic conversion of CO₂ to hydrocarbons by light-harvesting complex assisted Rh-doped TiO₂ photocatalyst," *Journal of CO₂ Utilization*, vol. 5, pp. 33–40, 2014.
- [15] O. Ozcan, F. Yukruk, E. U. Akkaya, and D. Uner, "Dye sensitized CO₂ reduction over pure and platinumized TiO₂," *Topics in Catalysis*, vol. 44, no. 4, pp. 523–528, 2007.
- [16] M. Subramanian, S. Vijayalakshmi, S. Venkataraj, and R. Jayavel, "Effect of cobalt doping on the structural and optical properties of TiO₂ films prepared by sol-gel process," *Thin Solid Films*, vol. 516, no. 12, pp. 3776–3782, 2008.
- [17] H. Žabová and V. Čírkva, "Microwave photocatalysis III. Transition metal ion-doped TiO₂ thin films on mercury electrodeless discharge lamps: preparation, characterization and their effect on the photocatalytic degradation of mono-chloroacetic acid and Rhodamine B," *Journal of Chemical Technology and Biotechnology*, vol. 84, no. 11, pp. 1624–1630, 2009.
- [18] J. A. Wang, R. Limas-Ballesteros, T. López et al., "Quantitative determination of titanium lattice defects and solid-state reaction mechanism in iron-doped TiO₂ photocatalysts," *Journal of Physical Chemistry B*, vol. 105, no. 40, pp. 9692–9698, 2001.
- [19] L. Laokiat, P. Khemthong, N. Grisdanurak, P. Sreearunothai, W. Pattanasiriwisawa, and W. Klysubun, "Photocatalytic degradation of benzene, toluene, ethylbenzene, and xylene (BTEX) using transition metal-doped titanium dioxide immobilized on fiberglass cloth," *Korean Journal of Chemical Engineering*, vol. 29, no. 3, pp. 377–383, 2012.
- [20] Z. Ambrus, N. Balázs, T. Alapi et al., "Synthesis, structure and photocatalytic properties of Fe(III)-doped TiO₂ prepared from TiCl₃," *Applied Catalysis B: Environmental*, vol. 81, no. 1–2, pp. 27–37, 2008.
- [21] K. Nagaveni, M. S. Hegde, and G. Madras, "Structure and photocatalytic activity of Ti_{1-x}M_xO_{2±δ} (M = W, V, Ce, Zr, Fe, and Cu) synthesized by solution combustion method," *The Journal of Physical Chemistry B*, vol. 108, no. 52, pp. 20204–20212, 2004.
- [22] Japan Society of Mechanical Engineering, *Heat Transfer Handbook*, Maruzen, Tokyo, Japan, 1st edition, 1993.
- [23] A. Nishimura, G. Mitsui, K. Nakamura, M. Hirota, and E. Hu, "CO₂ reforming characteristics under visible light response of Cr- or Ag-doped TiO₂ prepared by sol-gel and dip-coating

- process," *International Journal of Photoenergy*, vol. 2012, Article ID 184169, 12 pages, 2012.
- [24] Z. Goren, I. Willner, A. J. Nelson, and A. J. Frank, "Selective photoreduction of $\text{CO}_2/\text{HCO}_3^-$ to formate by aqueous suspensions and colloids of Pd-TiO₂," *Journal of Physical Chemistry*, vol. 94, no. 9, pp. 3784–3790, 1990.
- [25] I.-H. Tseng, W.-C. Chang, and J. C. S. Wu, "Photoreduction of CO₂ using sol-gel derived titania and titania-supported copper catalysts," *Applied Catalysis B: Environmental*, vol. 37, no. 1, pp. 37–48, 2002.
- [26] A. Nishimura, N. Sugiura, M. Fujita, S. Kato, and S. Kato, "Influence of preparation conditions of coated TiO₂ film on CO₂ reforming performance," *Kagaku Kogaku Ronbunshu*, vol. 33, no. 2, pp. 146–153, 2007.
- [27] A. Nishimura, N. Komatsu, G. Mitsui, M. Hirota, and E. Hu, "CO₂ reforming into fuel using TiO₂ photocatalyst and gas separation membrane," *Catalysis Today*, vol. 148, no. 3-4, pp. 341–349, 2009.
- [28] A. Nishimura, Y. Okano, M. Hirota, and E. Hu, "Effect of preparation condition of TiO₂ film and experimental condition on CO₂ reduction performance of TiO₂ photocatalyst membrane reactor," *International Journal of Photoenergy*, vol. 2011, Article ID 305650, 14 pages, 2011.
- [29] G. Marci, E. I. García-López, and L. Palmisano, "Photocatalytic CO₂ reduction in gas-solid regime in the presence of H₂O by using GaP/TiO₂ composite as photocatalyst under simulated solar light," *Catalysis Communications*, vol. 53, pp. 38–41, 2014.
- [30] G. Song, F. Xin, J. Chen, and X. Yin, "Photocatalytic reduction of CO₂ in cyclohexanol on CdS-TiO₂ heterostructured photocatalyst," *Applied Catalysis A: General*, vol. 473, pp. 90–95, 2014.
- [31] G. Song, F. Xin, and X. Yin, "Photocatalytic reduction of carbon dioxide over ZnFe₂O₄/TiO₂ nanobelts heterostructure in cyclohexanol," *Journal of Colloid and Interface Science*, vol. 442, pp. 60–66, 2015.
- [32] K. Oganisian, A. Hreniak, A. Sikora, D. G. Koniarek, and A. Iwan, "Synthesis of iron doped titanium dioxide by sol-gel method for magnetic applications," *Processing and Application of Ceramics*, vol. 9, no. 1, pp. 43–51, 2015.
- [33] J. P. Xu, L. Li, L. Y. Lv et al., "Structural and magnetic properties of Fe-doped anatase TiO₂ films annealed in vacuum," *Chinese Physics Letters*, vol. 26, no. 9, pp. 097502-1–097502-4, 2009.
- [34] K. J. Kim, Y. R. Park, and J. Y. Park, "Room-temperature ferromagnetic properties of Fe-doped TiO₂- δ thin films," *Journal of the Korean Physical Society*, vol. 48, no. 6, pp. 1422–1426, 2006.

